Applied Magnetic Resonance (2025) 56:229–252
https://doi.org/10.1007/s00723-024-01725-0

Applied
Magnetic Resonance

ORIGINAL PAPER

Performance Comparison of Different Rapid Freeze–Quench Strategies for Electron Paramagnetic Resonance

Maruan Bracci[1,2] · Ilenia Serra[1,2,4] · Inés García-Rubio[1,3] · Sabine Van Doorslaer[2]

Received: 14 July 2024 / Revised: 12 October 2024 / Accepted: 3 November 2024 /
Published online: 15 November 2024

Abstract

This work addresses the development of a custom-made home-built rapid freeze–quench (RFQ) device and the comparison of its performance to the one of a commercial RFQ setup that was in-house custom adapted. Both systems consist of two syringes that push the reactants into a mixing chamber and the products to a subsequent freezing setup. Using the binding of azide to myoglobin as a calibration reaction, the quenching times of the different setups were compared, evaluating different instrumental parameters, such as software-controlled variation of the aging time, variations of the flow rate and variations of the distance travelled by the mixed sample before freezing. In addition to minimal sample consumption, the home-built RFQ device was found to lead to the shorter reaction times which could be controlled in a time range from 10 to 25 ms. The commercial RFQ system yielded optimal reaction control in a time range from 50 to 200 ms, although a larger volume of reactants needed to be used due to the significant dead volume of the system. Three different freezing methods were also evaluated, among which, in our hands, freezing the jet directly in a deep bath of cold isopentane yielded shorter and reproducible freezing times.

✉ Inés García-Rubio
inesgr@unizar.es

✉ Sabine Van Doorslaer
sabine.vandoorslaer@uantwerpen.be

[1] Departamento de Física de La Materia Condensada, Universidad de Zaragoza, C/Pedro Cerbuna 12, 50009 Saragossa, Spain

[2] Department of Chemistry, TSM2 lab, University of Antwerp, Universiteitsplein 1, 2610 Antwerp, Belgium

[3] Instituto de Nanociencia y Materiales de Aragón (INMA), CSIC-Universidad de Zaragoza, 50009 Saragossa, Spain

[4] Present Address: Laboratory of Bioenergetics and Protein Engineering, CNRS/AMU, Marseille, France

1 Introduction

In the study of enzymatic reactions, the characterization of short-lived intermediate states can provide useful mechanistic insights. During their turnover, enzymes (*e.g.* heme enzymes) undergo transient spin and/or redox state changes which, when paramagnetic, are ideally investigated by EPR. However, the EPR signal from transition-metal ions, such as the ferric iron ion in heme systems, can be observed only at cryogenic temperatures due to fast electronic relaxation processes. For this reason, an issue emerges in the preparation of samples for EPR spectroscopy in case of fast reacting species. The manual procedure of mixing reactants and subsequent flash freezing in liquid nitrogen cannot be performed in milliseconds, which is often the time scale of enzymatic reactions. To overcome this experimental limitation, the technique of rapid freeze–quench (RFQ) was introduced in the 1960s [1]. The concept is analogous to the stopped-flow technique used in spectrophotometry, but in this case, after the mixing step, the sample is sent in the form of a fine jet from an ejection nozzle into a cryogenic bath or onto a cold metallic surface. The goal is to quench the reaction by freezing in the shortest time possible. Despite the simplicity of the idea, the practical use and optimization of the freeze–quench technique is not trivial. Several factors impact the achievable freezing time, the reproducibility of the experiment and the quality of the prepared sample.

Many of the aspects which still represent a challenge for RFQ applications nowadays, were already discussed in the seminal work of Bray [1], in which a model for an RFQ apparatus (then termed "thermal quenching") was proposed for the first time. The system consisted of a constant-speed hydraulic ram which drove the reagents syringes. The solutions would then meet into a mixing chamber and exit, through a 0.5-mm diameter-wide jet tube, onto the surface of cold hexane or isopentane. In the same work, the author elaborates on the methods to provide an efficient mixing and freezing of the reagents, emphasizing the importance of using a small ejection nozzle (theoretically optimal when < 0.2 mm) to obtain small droplets and, consequently, a fast cooling. In an addendum, Bray and Pettersson [2] describe the development of a collection system to pack the frozen particles into a tube suitable for EPR spectroscopy measurements. From an initial sample volume of 0.3–0.5 mL, they obtained a solid mass about 2 cm in height of a 4-mm ID X-band tube of which ~ 60% was estimated to be ice. They reported freezing times of 5–6 ms. Later on, several improvements were proposed to the device introduced by Bray [3, 4]. In 1974, Ballou and Palmer provided a detailed description and evaluation of the evolved version of that original freeze–quench device [5]. As it was already discussed in the earlier works, also Ballou and Palmer highlighted the influence of factors such as the flow rate or the diameter of the ejection nozzle on the quality of the obtained sample. In particular, the main issue appeared to be the homogeneity of the frozen particles and the packing efficiency inside the EPR tube. In fact, the authors reported a loss of intensity of the EPR signal of the freeze-quenched sample compared to a standard freezing of the liquid sample in the tube, presumably due to a packing efficiency of only

about 50–70%, which constituted for them an important uncertainty in determining the quenching time. As a calibrating reaction they used the well-known binding reaction of azide (N_3^-) to ferric myoglobin (Mb), which has been ever since considered as a standard for calibration of RFQ devices.

The commercialization of the RFQ instruments in the 1990s led to its growing popularity in enzyme research. Different sample collection systems were adapted to be coupled to NMR [6], EPR [7] and Mössbauer [8] spectroscopies, even though the freezing method was still based on fast spraying into a bath of cold isopentane or propane. In 2000, Oellerich et al. presented a method for collecting the freeze-quenched sample in a way that it could be sequentially investigated by EPR and Resonance Raman spectroscopies [9]. While their device and freezing method were essentially similar to the ones already described in literature, these authors strongly highlighted the limited reliability of the commonly used calibration procedure to determine the quenching time, which, as for the previous devices, was based on free myoglobin quantification (high-spin Fe^{3+}). In line with the observations made during the development of earlier RFQ setups, they emphasized the struggle to obtain a good packing efficiency and reproducibility, which reflected on the poor fitting of the calibration curve obtained by EPR experiments.

In the attempt to overcome the limitations of the commercial setups and to achieve a faster freezing, several research groups turned once again to home-made RFQ devices. A new approach, first introduced by Tanaka and colleagues [10] and later followed by Lin et al. [11], was based on spraying the sample directly on the surface of rotating metal disks (made out of copper or silver) partially submerged in liquid nitrogen. In this way, a fine powder of frozen sample particles was directly transferred by the rotating disk into the liquid nitrogen underneath. In combination with the use of high-performance sub-millisecond micro-mixers, this method provided quenching times of ~ 50–200 μs. A more sophisticated solution was later developed by Cherepanov and de Vries [12], who described a microsecond freeze-hyper-quenching device and reported a total quenching time of ~ 130 μs. In their system, HPLC-grade pumps and tubing are used to apply high-pressures and obtain high linear flow rates. The reagents are injected into a tangential micro-mixer which guarantees a mixing time < 20 μs and efficiently mixes viscous aqueous solutions. Both the mixer and the collection system are mounted in a low-pressure chamber to maintain the jet speed between the mixer and the freezing medium constant. A small jet diameter and a high jet speed allow a freezing time < 30 μs. Other groups used a similar setup in combination with spin-label EPR (dipolar spectroscopy) or solid state nuclear magnetic resonance (ssNMR) to study folding and conformational changes in biomolecules [13–17].

Due to the better *g*-factor resolution at high-frequency EPR, RFQ can be coupled with such technique (*e.g.* at W-band, ~ 94 GHz) to study reaction intermediates containing organic radicals. However, the small size of the sample holders (for about ~ 2–4 μL of sample) complicates sample collection. In 2004, Schünemann and colleagues reported the first application of RFQ to high-frequency EPR with the use of a commercial device coupled to a home-made sample collection system adapted to the W-band EPR capillaries immersed in isopentane [18]. In another application from Manzerova et al. [19], several innovative parts were designed and assembled.

First, the ejection nozzle consisted in a metal tube bent at a 90° angle having 25 drilled holes, 100 µm in diameter, to break the stream into independent jets of high kinetic energy. Secondly, the freezing method based on the work of Tanaka et al. and Lin et al. [10, 11], was upgraded with the use of a copper-beryllium alloy for the rotating disk, to retain the thermal conductivity of copper and having at the same time a more resistant material to allow abrasive scratching. An ingenious way to scrape the frozen powder off the disks was employed by bringing single-edged blades into contact with the rotating wheels. Finally, an adapted packing procedure was designed to fill the small capillaries necessary for D-band EPR (~140 GHz). A similar approach has been used by Kaufmann et al. [20] to prepare freeze–quenched samples for W-band EPR, but with their setup it was possible to collect samples quenched at different times in a single freezing experiment. For high-field EPR, concerns have been raised about the use of the myoglobin-azide reaction for calibration, due to the line broadening of the spectra and the costs associated to the large amount of helium consumed to scan a very broad field range [21]. Alternatively, a calibration method relying on the reduction of a nitroxide radical in presence of Mn^{2+} was proposed as a standard [21]. Nevertheless, the reaction of myoglobin with azide was successfully applied for RFQ-EPR measurements at 275 GHz, where only the low field feature of the high-spin Fe^{3+} was recorded, and the normalization performed with the aid of a Mn^{2+} reference signal [22].

One of the major drawbacks in the application of the freeze–quench technique to biological samples is the typically high amount of sample needed per single experiment, which results from inefficient sample collection and packing, and from the large dead volume of some of the systems. Considerable efforts in the optimization of the amount of sample required for RFQ applications have been made by the group of E. Groenen. First, they described an improved way of collecting freeze–quench particles from isopentane [23] which made use of X-band EPR tubes with an open end tapered with a polypropylene filter disk. To efficiently pack the frozen particles in the tube, and remove the excess of isopentane, they applied an aspiration at the open end of the tube. It has to be noted that this method was a re-adaptation of a solution earlier proposed by Tsai and colleagues [24], in which similarly tapered open-end tubes were used, with the difference that the packing was obtained by applying a positive nitrogen gas pressure from the top of the tube. While the method described by Tsai et al. was finally evaluated to have a packing efficiency of 0.45–0.5 [24], the collection system proposed by Nami et al. showed an improved efficiency of 0.68–0.76 [23]. Later, Groenen and colleagues further developed their packing system to adapt it to the coupling of RFQ with high-frequency EPR [22], demonstrating that only a single series of RFQ samples is needed for multi-frequency EPR (9.5 GHz and 275 GHz). To finish the inspiring collection of previous RFQ devices—which should not be intended as an exhaustive review of the available RFQ literature—we highlight the construction of a mixing device which couples optical stopped-flow measurements and RFQ that was recently developed by Bujnowicz and colleagues [25]. By allowing the combination of different spectroscopic techniques in a single experiment, their setup not only requires a less amount of sample, but also provides an interesting application for the full characterization of (bio) chemical reactions.

It is clear from the above examples that despite many instrumental developments and uses of RFQ in spectroscopic applications, the technique remains challenging because it is difficult to combine in one device all properties of the ideal RFQ apparatus, that is, fast and controllable reaction time and minimal sample consumption through optimized sample collection and packing and low dead volume. In this work, we describe the development of a sample-sparring custom-made home-built RFQ system and compare its performance with an in-house adapted version of a commercially available RFQ system. Both systems consist of two syringes that push the reactants into a mixing chamber and then push the products to the freezing stage. Moreover, three different technical variants for freezing and collecting of the sample are evaluated. We focus in detail on the mixing, transport and freezing times to optimize and control the RFQ process. Different methods to control the reaction time were evaluated: software-controlled variation of the aging time, variations of the flow rate and variations of the distance travelled by the mixed sample before freezing.

We use the reaction between myoglobin and sodium azide with X-band continuous wave (CW) EPR as a standard for the calibration procedure [5, 9, 26], which is changed from the one of the first reports in a crucial aspect. Here we not only quantify free myoglobin (high-spin), but also azide-bound myoglobin (low-spin). Since the ratio between both species is a fingerprint of the reaction time [23, 26], this calibration procedure makes the determination of the quenched reaction time independent of the success of the procedure of sample collection and packing.

2 Materials and methods

2.1 Materials

Myoglobin (Mb) from horse skeletal muscle (95–100% pure, essentially salt-free lyophilized powder), TRIS, sodium azide (NaN_3) NaH2PO_4 and peracetic acid (PA) were purchased from Sigma Aldrich. For RFQ purposes, the lyophilized Mb powder was dissolved directly in 100 mM Tris–HCl buffer, pH 7 to a concentration of 1 mM Mb. 5 mM, 9.5 mM and 30 mM solutions of sodium azide in MilliQ water were prepared. For the kinetics analysis with stopped-flow optical spectroscopy, concentrations of 1.5 µM Mb and 175 µM azide were used. All the experiments were performed using a 1:1 volume ratio of the Mb and azide solutions. The total volume of the sprayed solution varied depending on the RFQ apparatus, but in general it was kept between 150 and 300 µL per sample.

Chloroperoxidase was produced as extracellular glycosated enzyme from the fungus *Caldariomyces fumago* [27] with the microorganism produced using the method described in reference [28]. A 100 mM NaH_2PO_4 buffer of pH 4.5 was used.

2.2 Commercial RFQ System

As a basis for the first RFQ setup (see Sect. 3.1) a commercial device from BioLogic was used, composed of an SFM-2000 stopped-flow unit and an MPS-70 controller

unit coupled with a freeze-quench accessory (catalogue n. 053-11/10). The schematic diagram of the system and its working are reported in Fig. S1 and Section S1, supplementary material.

2.3 Spectroscopy

Continuous wave (CW) EPR spectra were recorded with an X-band ELEXSYS E580 spectrometer (Bruker BioSpin, GmbH) operating at a microwave frequency of ~ 9.4 GHz and equipped with a standard TE102 cavity and a liquid He cryostat (Oxford Inc.) for both the experiments coupled with the commercial RFQ set-up (University of Antwerp) and the experiments coupled with the home-built RFQ system (University of Zaragoza). Measurements were performed at 10 K under non-saturating conditions with a magnetic field modulation of 1 mT and 100 kHz.

For the kinetics measurements, a stopped-flow spectrophotometer from Applied Photophysics (SX.18MV, Applied Photophysics Ltd., Leatherhead, UK) interfaced with a photodiode array detector was used.

2.4 Jet speed and Reynolds Number Calculations

Depending on its velocity, the flow of a liquid in a tube can be laminar when the fluid moves in parallel layers (low velocity) or turbulent, when the flow swirls irregularly and mixes chaotically (high velocity). The Reynolds number is a dimensionless parameter used to evaluate the flow regime:

$$R_e = \frac{\overline{u} \cdot d}{v_k} \tag{1}$$

where $\overline{u}$ is the average velocity of the flow (jet speed), d is the inner diameter of the circular section of the tube and v_k is the kinematic viscosity of the fluid.

If R_e exceeds the critical value of 2300, the flow is considered turbulent; otherwise, it can be considered laminar [29]. For the calculations presented in this work, the approximated kinematic viscosity for water at 20 °C was taken, *i.e.* 1 mm^2/s.

For both flow regimes, the volumetric flow rate F is defined as the volume of fluid that goes through a given section per unit time. It can be written in terms of the average speed of the flow and the inner diameter of the tube as:

$$F = \overline{u} \cdot \pi \frac{d^2}{4} \tag{2}$$

2.5 Reaction Time in RFQ

When two reactants are mixed in an RFQ device, the whole reaction time t_q can be split in several contributions, some of which can be controlled in the RFQ devices used in this study [6]. The different contributions are the mixing time (t_m), aging time (t_a), transport time (t_t) and freezing time (t_f) [12]

$$t_q = t_m + t_a + t_t + t_f \tag{3}$$

t_m depends mainly on the geometry of the mixer and its physical properties [30, 31]. In this work, we have estimated this time from the mixer volume and the flow rates. t_a is a delay time artificially introduced by the user in the commercial pump setup from BioLogic, which is obtained by stopping the flow by the desired period of time. An equivalent aging time was not implemented in the home-built setup. t_t is the time needed to transfer the sample from the outlet of the mixer to the surface of the quenching system. This transport time can also be theoretically calculated, on average, using Eq. 2 for turbulent flows taking into account the flow rates, the diameter and length of the tubes and the distance from the nozzle to the quenching surface. Particular care should be taken in the calculation of t_t in the case of laminar flows ($R_e < 2300$), since in that case the speed of each layer is different, following a parabolic distribution of speeds depending on the distance to the tube walls, as formulated in Navier–Stokes equations [32]. One has to take into account that $\overline{u}$ in Eq. 2 is the average velocity of the whole tube section. Finally, t_f is the time needed to completely freeze the sample and stop the reaction. This value is hard to estimate theoretically because it depends on factors like the size and shape of the particles, the heat transfer coefficients, the sample latent heat, the contact surface area and all the temperatures involved in the process at a quasi-microscopic scale [26]. Therefore, it would be very interesting to experimentally determine the freezing time by a calibration procedure of the RFQ operation. To do so, calibration datasets have been measured in which the different data points were obtained varying t_a or t_t in a controlled way.

2.6 RFQ Calibration

The most common procedure to test the performance of the RFQ coupled with EPR is using the azide-binding reaction to ferric myoglobin (Mb) [5, 9, 22, 26]. In ferric Mb or aquomet Mb the heme iron is bound to a histidine residue on the proximal side and a water molecule on the distal side, leading to an EPR-signal characteristic of a high-spin (HS) Fe(III) heme form (Fig. S3, supplementary material). When the strong base azide replaces the distal water ligand, the EPR signature of a low-spin (LS) ferric heme form appears (Fig. S3, supplementary material). This binding reaction becomes (pseudo) 1st order, when a large excess of azide is used. The detailed calibration procedure is given in the supplementary material (section S2). Briefly, the quenching time t_q can at all times be written as

$$t_q = t = -\frac{\ln(N(t))}{k'} = -\frac{\ln\left(\frac{R_t}{R_t+\lambda}\right)}{k'} \tag{4}$$

in which k' is the apparent first-order rate constant. R_t is the ratio of the signal intensity (I) of the HS and LS EPR features at time t (see section S2, supplementary material)

$$R_t = \frac{\left(I_{HS}\right)_t}{\left(I_{LS}\right)_t}, \tag{5}$$

and λ is the ratio of the intensity of the EPR signal of the HS species at $t=0$ (start of the reaction) and the intensity of the EPR signal of the LS species at the end of the reaction ($t=\infty$)

$$\lambda = \frac{\left(I_{HS}\right)_0}{\left(I_{LS}\right)_\infty} \tag{6}$$

Since the quenching time t_q is the sum of the unknown freezing time t_f and the times t_m, t_t and t_a that can be estimated for every experiment (Eq. 3), linear fitting of $-\ln(N(t_q))$ versus $t = t_t + t_a + t_m$ allows the experimental determination of the freezing time as the time point at which the line intercepts the time axis. From the slope of the line, the determination of *k'*-values from the EPR data can be obtained. As a control, *k*'-values were also determined using stopped-flow spectrophotometry (section S2, supplementary material).

3 Design, Adaptation and Operation of Rapid Freeze Quench Setups

3.1 System 1: In-House Adaptation of Commercial RFQ Apparatus

In the standard working scheme of the BioLogic RFQ setup (Fig. S1), the products are, after mixing, transferred through a loop called an ejection delay line (EDL) to a nozzle with internal diameter of 0.5 mm and sprayed to the surface of cold isopentane. Five exchangeable EDLs used to age the sample are available with different volumes. The volumes of each component are reported in Table S1 of the supplementary material. Considering that the smallest EDL has a volume of 12.4 µL, the minimum dead volume of the instrument is 521 µL. To lower the amount of sample required to operate this system and improve the performance of the instrument, a custom-made EDL and nozzle were manufactured (Table S1, Section S1).

One of the main advantages of this apparatus is that the reaction time can be conveniently controlled. This can be done in two different ways. In the *first method* the syringes move continuously with no interruptions. To achieve different aging times, the flow rate is adjusted according to the desired reaction time (see Eq. 2): for a given ejection line (nozzle), the faster the flow speed is, the shorter the time elapsed between mixing the reactants and spraying the products out of the nozzle (t_t). In Table 1 the calculated average-flow velocities and transport times are reported for both home-made and commercial EDLs and different flow rates. A *second method* to change the aging time consists in storing the sample for a controlled amount of time in the installed EDL after mixing. Once the reactants are mixed, the syringes stop for the desired time (aging time t_a) before pushing the mixture out into the isopentane bath. A convenient graphical user

Table 1 Calculated values for the flow velocity, average transport time and Reynolds number in the BioLogic commercial RFQ system. The values for the average jet speed $\overline{u}$ were calculated using Eq. 2 for the commercial and custom-made EDLs. The Reynolds number (R_e) was calculated using Eq. 1

Flow rate (F) [mL/s]	Jet speed ($\overline{u}$) [mm/ms]	Average transport time (t_t) [ms/cm]	R_e
Commercial EDLs. Ejection nozzle of ID = 0.5 mm			
1	5.1	1.96	2,550
4	20.4	0.49	10,200
6	30.6	0.33	15,300
8	40.8	0.24	20,400
10	50.9	0.20	25,450
Custom-made EDL. Ejection nozzle of ID = 0.3 mm			
1	14.1	0.71	4,230
4	56.6	0.18	16,980
6	84.9	0.12	25,470
8	113.2	0.09	33,960
10	141.5	0.07	42,450

interface provided by the control software makes it easy to set up parameters such as flow rates, aging times, and injection volumes.

The freezing stage of this commercial device consists simply of a tempering dewar flask (type TSS-G from KGW Isotherm) containing cold isopentane. For a better stability and control of the isopentane temperature, a home-made cooling system was designed and incorporated to upgrade the freezing procedure of the sprayed samples. A standard cylindrical vacuum-glass dewar flask (type C from KGW Isotherm) was filled with isopentane and cooled with a custom-made system composed by two copper coil tubes (outer diameter (OD) = 4 mm) designed for piping a nitrogen gas flow (Fig. 1a). One of the coils is immersed in a dewar containing liquid nitrogen and the other coil in the dewar with isopentane (see Fig. 1b). The temperature of isopentane is constantly monitored with a thermocouple just below the surface and can be controlled by varying the flow of the nitrogen gas through the coils: higher flows produce lower temperatures in the isopentane bath. For optimal operation, the flow was regulated to maintain the bath at a constant temperature of −120 °C. For further ease of use, the quenching and cooling systems were mounted in a home-made sliding plate that can be conveniently moved from the position in which the sample is sprayed (under the freeze quench accessory) to the position in which the sample is collected (open air position to allow manipulation). The distance between the outlet nozzle and the isopentane bath was always kept as short as possible (40 mm).

Sample collection makes use of a funnel made out of PTFE (polytetrafluoroethylene) (EPR/NMR model, see Fig. S2) provided by BioLogic to be placed into the isopentane bath. The holding clips of the funnel have been adapted to fit inside the cooling copper coil at the desired height. EPR quartz tubes (~ 125 mm length) were connected to the bottom of the funnel. After freezing the reaction products into the isopentane, the particles are gently moved to the EPR tube

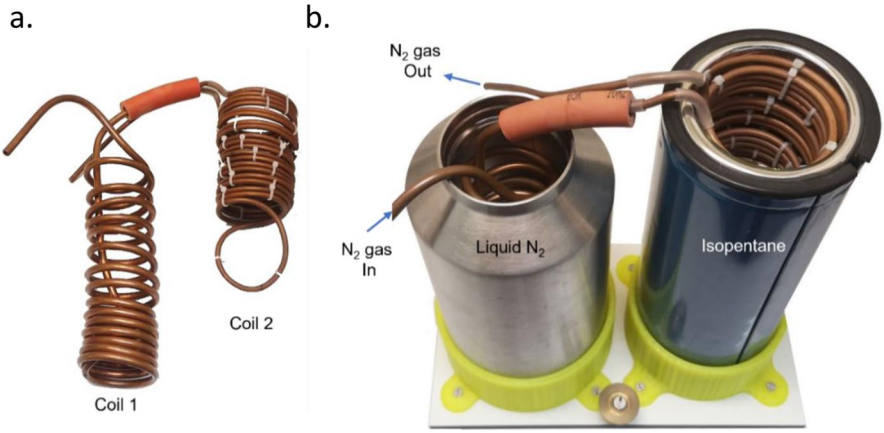

Fig. 1 Custom-made isopentane cooling system. a. Copper coils used to circulate nitrogen gas. The flow can be controlled with a valve not shown in the picture. Coil 1 is immersed in liquid nitrogen, coil 2 is immersed in isopentane. b. Coils and dewars. The metal dewar is filled with liquid nitrogen and refilled periodically. The glass dewar is filled with isopentane and the temperature is monitored with a thermocouple. Both dewars are mounted in a sliding plate especially designed to improve handling and stability of the system

using a metal stick with a PTFE head provided with the instrument and packed as tightly as possible inside the EPR tube.

In our experience, this system is robust and provided with convenient software and can be used to produce freeze–quenched samples at desired reaction times. On the other hand, the main drawback found when operating this system is the high amount of reagents needed for the preparation of one sample, which is on the order of milliliters, since the minimum dead volume of the instrument is about 520 µL. Transferring the reactants from the loading syringes to the built-in syringes of the apparatus further increases the total dead volume of the system. With some skill from the operator, part of that volume can be recovered from the tubing before the mixer, but there remains a large consumption of protein that is in many cases not desired or even affordable.

3.2 System 2: A Home-Made Rapid Freeze–Quench Device with Silver Rods

To be able to reduce the dead volume and, ultimately, the amount of sample needed for one experiment, as well as to decrease the freezing time, a new system was designed with the priority of having a low volume mixer and small diameter tubing and nozzle, to spare sample consumption and produce a thin jet that can reduce freezing times. In this system the reactants are loaded into two 1-mL air-tight glass syringes equipped with Luer-lock connections and mounted directly in a stand-alone syringe pump (see Fig. 2a). The pump pushes simultaneously the plungers of both syringes by a ram driven by a step motor whose speed can be controlled. The accessible flows for this setup are reported in Table 2. The reactants are pushed through

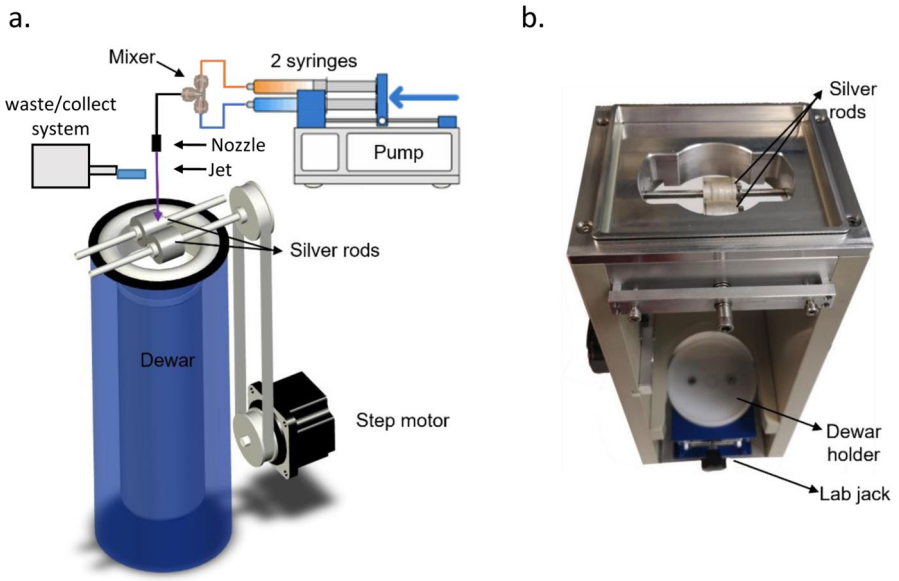

Fig. 2 Home-made freeze–quench device. **a** Schematic representation of the RFQ apparatus. A syringe pump pushes simultaneously the two syringes with the reactants, which are mixed in the micro-static mixing tee. The products are sprayed through a nozzle directly onto the surface of one of two spinning silver cylinders kept at liquid nitrogen temperature. A waste/collect switch allows for the reduction of sample waste. **b** Photograph of the device. A dewar flask is placed on the white disk that serves as dewar support. The height of the dewar is controlled with the lab jack. The pump system, the control unit of the speed of the rods and the dewar are not shown in the picture

two 90-mm-long connecting capillary tubes made of PEEK (polyether ether ketone) with an inner diameter (ID) of 254 µm into a micro static mixing tee assembly. The mixing block is entirely built with standard HPLC materials able to withstand high pressures and is connected to an outlet spraying nozzle. The volumes and dimensions of the components are reported in Table 3. Two different low-volume commercial mixers from Idex Health and Science were used with the system, one is provided with a mixing frit (model M-540) and a second one, without the frit, with a slightly larger volume (model M-540A). The nozzle is a carefully rounded termination of a 17 mm long PEEK tube connected to the outlet of the mixer. Several internal diameters have been tested for the outlet tube, see Table 2. The average speed of the sprayed jet was calculated using Eq. 2 for every flow-rate and nozzle diameter (Table 2). In this case, the flow can be considered laminar (see Reynolds numbers lower than 2300 in Table 2) and therefore the calculated speed is an average of the parabolic distribution of speeds generated in the jet. In the supplementary material (Section S3), an analysis of the effects of the laminar speed distribution on the estimated freezing times is presented. The $R_e > 2300$ reported in Table 2 are not accessible with the pump described here, since the backpressure generated by the narrowest capillary tube is too high and it could only be operated at the slowest speed with the thinnest outlet tube. The distance between the nozzle and the cryogenic surface was always kept as short as possible (about 25 mm).

Table 2 Five representative accessible flow rates using the home-made pump system. The minimum and the maximum flow rates are dictated by dripping of the mixture and the power of the pump, respectively. Average jet speeds and transport times were calculated using Eq. 2 for three different nozzle diameters. The most used nozzle has an ID of 0.127 mm, for which the trade-off between back-pressure and jet speed was found to be optimal. The average jet speed is considered a valuable number, since the instrument works mainly in laminar flow condition (R_e is less than 2300 for the middle and larger tubes)

Flow rate (F) [mL/s]	Average jet speed ($\bar{u}$) [mm/ms]	Average transport time (t_t) [ms/cm]	R_e
Ejection nozzle of ID = 0.05 mm			
0.017	8.5	1.18	425
0.062*	31.8	0.31	1,589
0.093*	47.3	0.21	2,364
0.123*	62.8	0.16	3,140
0.154*	78.3	0.13	3,916
Ejection nozzle of ID = 0.127 mm			
0.017	1.3	7.58	167
0.062	4.9	2.03	625
0.093	7.3	1.36	931
0.123	9.7	1.03	1,236
0.154	12.1	0.82	1,542
Ejection nozzle of ID = 0.254 mm			
0.017	0.3	30.3	84
0.062	1.2	8.12	313
0.093	1.8	5.46	465
0.123	2.4	4.11	618
0.154	3.0	3.29	771

*Flow-rate values not accessible in the experimental setup due to excessive backpressure

Table 3 Volumes of the transport and mixing components for the home-made freeze–quench setup

Component		Volume [μL]	Length [mm]
Syringes		1000 each	
Connections (ID 0.245 mm)		4.6 each	90
Mixer	With frit	0.95	
	Without frit	2.2	
Ejection line	ID 0.05 mm	0.03	17
	ID 0.127 mm	0.22	17
	ID 0.254 mm	0.86	17

As mentioned above, the sample contained in the mixer and outlet tube from a previous experiment needs to be discarded before initiating the mixing process, hence, the first microliters of mixed solution of every shot are rejected. If this operation were performed manually, 40–60 μL of mixed solution would be thrown away. To reduce this unnecessary waste, an automatic switch from "waste" to "collect" positions was built into the system to clean the mixer and the nozzle from previously aged solution (see Fig. 3). When it is done with the automatic system, only approximately 10 μL are discarded to ensure that the mixer and nozzle are properly flushed.

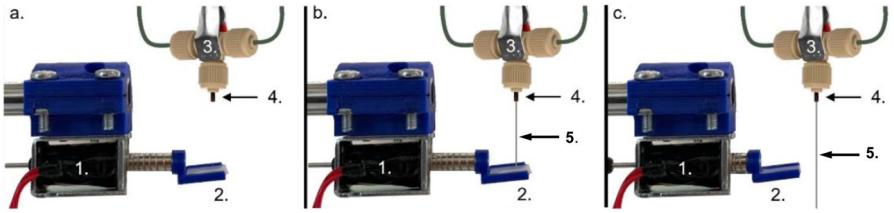

Fig. 3 Implementation of an automatic switch to discard the first microliters of sample exiting the nozzle. The switch is composed of a solenoid (#1) and a moving 3D-printed tray (#2) with absorbent paper which was designed to collect the first few µL of every sample mixture shot. **a** The system in resting position. The mixer is held in position by a clamp (#3). **b** The mixed solution is ejected from the nozzle (#4) in the form of a narrow jet (#5). The first few microliters are collected in the waste tray (#2). **c** The tray (#2) is moved aside, and the sample is then frozen and collected

The slit (#2 in Fig. 3) is connected to the solenoid (#1) that is triggered by the control system of the pump (Fig. 3a). The time elapsed between the slid-in waste position (Fig. 3b) and collect position (Fig. 3c) can be set by the user through a potentiometer with the scale calibrated in milliseconds.

This loading and mixing system was coupled to a home-made freeze–quench device inspired by the one reported in reference [11]. The freezing surfaces are the sides of two 2 cm diameter silver cylinders in contact with each other as shown in Fig. 2. One of the wheels is moved by a step motor with controllable speed. The motion is transferred to the other cylinder by frictional contact. As a result, the two silver cylinders rotate at the same speed and in opposite directions. The silver blocks are cooled by a bath of liquid nitrogen into which they are half immersed to keep their temperature at 77 K. The sample is then sprayed on the surface of one of them at a point that is convenient to prevent back-splash. The aim of this design was to shorten the freezing time of the sample due to the high thermal conductivity of the silver and its grinding into a fine powder due to the intimate contact with the other cylinder which would mash and freeze the mixture. Underneath the cylinders, a collecting funnel is placed into the liquid nitrogen (Fig. 4). With the help of a brass stick the frozen sample is collected into an EPR quartz tube connected to the bottom of the funnel.

As the device was completely home-made, every component was customized or adapted. The length of the outlet tube, which acts as an EDL, its internal diameter (diameter of the nozzle), the distance between the nozzle and the cryogenic surface, the volumes of the injection syringes could be easily changed at will. In this setup the tubing was kept as short as possible to reduce the dead volume as much as possible, in practice to about 10 µL. Also, the use of liquid nitrogen allows cooling of the silver rods to 77 K, lower than with isopentane.

Unfortunately, the immersion of the sample collection tool in liquid nitrogen makes the collection procedure longer. Since N_2 is liquid in a small temperature window from 63 to 77 K and the dewar is open to air, the boiling of the liquid N_2 contained in the funnel causes the small frozen particles to swirl and prevents the easy deposition in the EPR tube. Eventually, the effect of gravity brings the fine powder to the bottom of the tube.

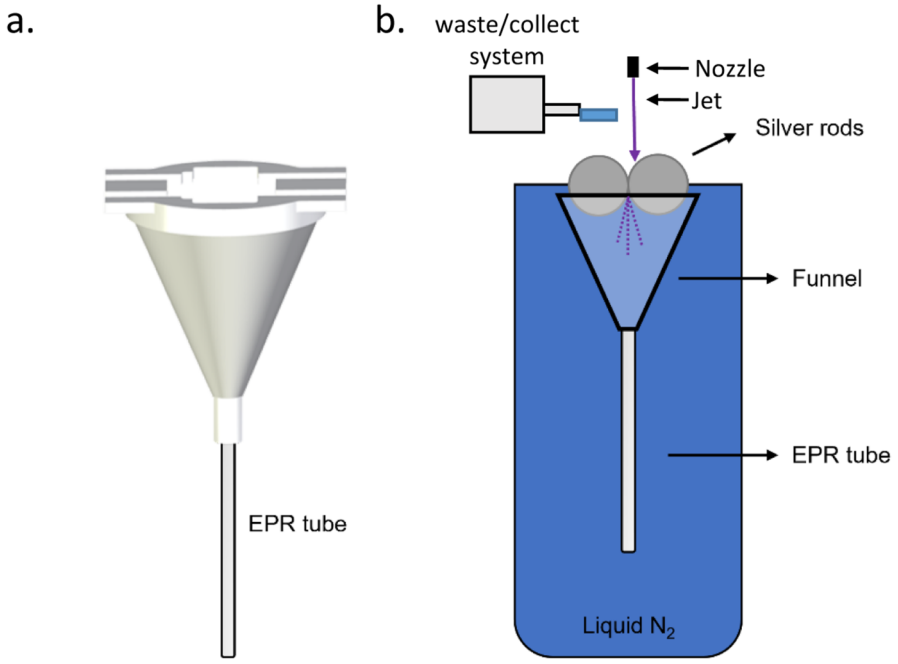

Fig. 4 Collection system. a. Side-view drawing of the PTFE funnel connected with the EPR tube. b. The products are sprayed from the nozzle, passing the waste/collect system (see Fig. 3) and finally reach the surface of a spinning silver rod. The jet is kept as close as possible to the silver surface and at a distance that does not allow the nozzle to freeze. After freezing, the particles are grinded and released into the funnel. The funnel is shown with semi-transparent walls. At the bottom, the funnel is connected to the EPR tube. The funnel-tube ensemble is placed inside the dewar filled with liquid nitrogen

3.3 System 3: Home-Made RFQ Device Coupled to a Deep Isopentane Bath

In this Section, a variant of the home-made device described above is presented, in which the same loading and mixing blocks are used but the freezing device is substituted by an isopentane bath (Fig. 5). This setup was standard operated with the mixer with no frit (model M-540A by Idex H&S) with a volume of 2.2 μL to prevent clogging problems that had been observed with the other mixer. The samples were sprayed directly into a 50 mL Falcon tube containing isopentane precooled at 153 K. Again, the distance from the nozzle to the isopentane surface was kept as short as possible at about 25 mm (see scheme in Fig. 5). Immediately after freezing the sample, the falcon is moved either to dry ice (195 K) or to a dewar containing a small amount of liquid nitrogen (77 K) to keep it at low temperature until completing the sample collection.

The frozen sample contained in the isopentane can then be transferred into an EPR tube using a precooled funnel as previously described. However, we found it more convenient to collect the sample using vacuum, as described by Nami et al. [23] and summarized below. To operate sample collection with this

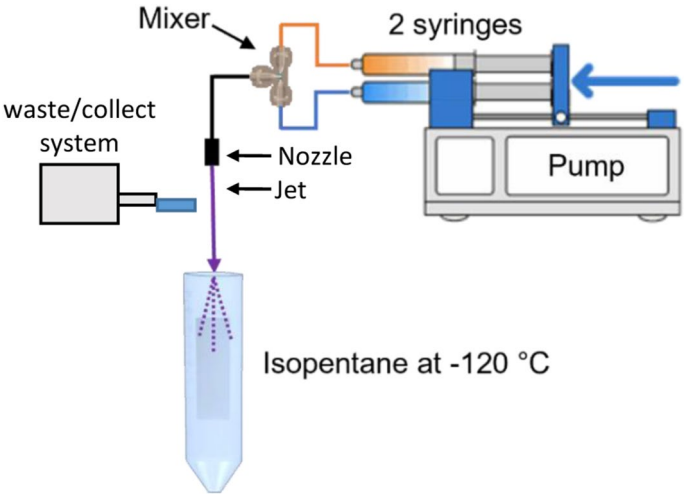

Fig. 5 Schematic illustration of the home-made RFQ device. The pump and mixing systems are the ones described previously. The freezing method consists of spraying through the nozzle passed the waste/collect system directly into a 50-mL plastic Falcon tube filled with cold isopentane. The frozen sample can be collected immediately. Alternatively, the isopentane tube containing the frozen sample can be stored in liquid nitrogen for future collection

procedure a quartz EPR tube of OD 4 mm and 150 mm length open on both sides was used. The entire length of the tube and one of the openings have an ID of 3 mm, the other end has a flaring that reduces the ID to 2 mm so that the tube is open on both sides, but one end is narrower than the other. A Mobicol filter from MoBiTec (product number M2190) with 90 µm pore size and diameter of 2.7 mm is inserted inside the EPR tube and held at the opposite end by the flaring of the walls. The narrower end is connected to lower pressure by a Venturi effect pump (water jet pump) and the other end is inserted into the cold isopentane containing the frozen sample. The cold liquid isopentane passes through the EPR tube and through the filter, cooling it down and is finally collected in a cold trap. Instead, the frozen particles are collected in the filter (Fig. 6). Before the isopentane runs out, the pump is stopped, and the quartz tube is disconnected from it. The outside walls are cleaned with a cold cloth to remove isopentane and the EPR tube is rapidly stored in liquid nitrogen. Note that due to the open-bottom EPR tube, extra care is necessary not to lose the content of the tube.

4 Performance of the RFQ Setups

Performance tests of the RFQ devices operated as described above were carried out according to the procedure specified in Sects. 2.6 and S2 (supplementary material) using the binding reaction of azide to ferric myoglobin. The aim of these tests was to determine:

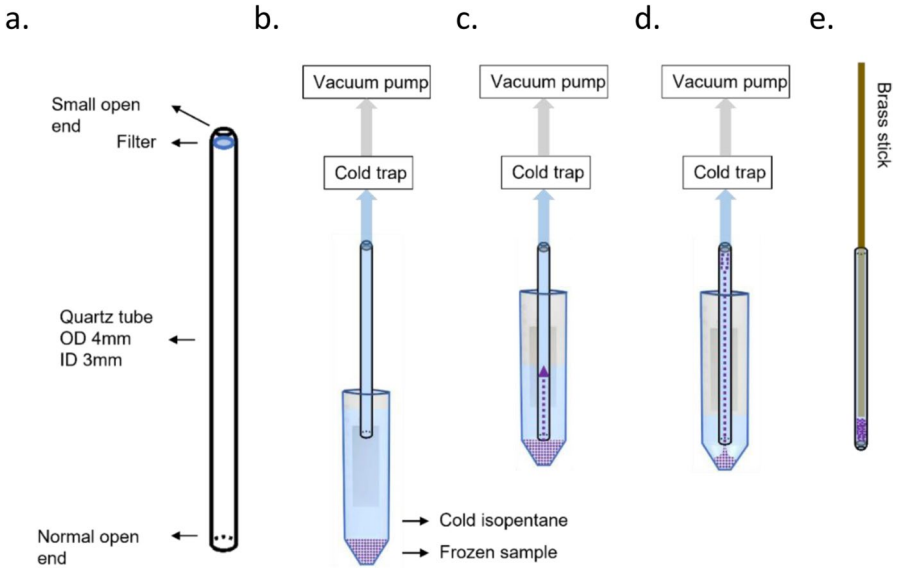

Fig. 6 Sample collection using a pump. **a** Quartz tube used for collecting frozen sample particles from cold isopentane. Both ends are open, but one has a flaring housing a 90-µm-pore-size filter. **b** The tube is connected to a cold trap to collect the isopentane and to a vacuum pump. The low pressure produced by the pump drives the cold isopentane contained in the 50 mL test tube. The top layer of isopentane is used to precool the quartz tube, as no sample is contained in that region. **c** The quartz tube is moved to the bottom of the test tube, where the sample has accumulated by gravity. **d** The small frozen particles are transported with the isopentane flow to the top of the tube where they are stopped by the filter. **e** The quartz tube is disconnected from the cold trap and the particles are compressed with a cold brass stick. The tube is immediately stored in liquid nitrogen. All the operations described must be done with the maximum care to prevent heating of the sample

1. The shortest reaction time that can be achieved with every device;
2. Whether the reaction time can be varied in a controlled way;
3. The apparent kinetic constant, *k'*, directly derived from the RFQ measurements. Since some of the reaction conditions at which the RFQ experiments were performed, such as pressure and protein concentration, differ significantly from the ones of stopped flow UV–Vis absorption experiments, variations in *k'* are possible.
4. The amount of required reactant volume needed to prepare one sample.

Depending on the setup, three different methods were used to control the reaction time:

a. using a software-controlled aging time (variation of t_a, only for the setup from BioLogic);
b. changing the flow rate (variation of $t_m + t_t$);
c. modifying the distance travelled by the mixed sample by changing the length of the outlet tube(variation of t_t).

For all three methods, the length of the EDL/outlet tube and its diameter, the mixer volume, and the ram velocity were used to compute average values for t_m and t_t.

4.1 Calibration of Commercial RFQ System 1

A first set of samples was prepared exclusively by varying the aging time (t_a) of the solution (grey circles in Fig. 7) mixed with a constant flow rate of 2 mL/s in the ejection line of 87.1 µL (EDL #3). This approach allows exploring reaction times longer than 55 ms, since the aging time was varied between 5 and 120 ms from the control software and the transport time plus the mixing time was 50.6 ms for the selected EDL and flow rate. The plot of the negative logarithm of $N(t_q)$ versus time ($=t_t+t_m+t_a$) is shown in Fig. 7. Each experimental point is the average of the measurement of at least three different samples, the error bars represent their standard deviation. The trend of the data is clearly linear in this region, according to Eq. 4, the slope is the reaction rate k'. The best linear fit for the data points ($R^2=0.99$) yields an apparent pseudo first-order slope of $k' = k\left[N_3^-\right] = 15.14 \pm 1.43\ s^{-1}$, which, taking into account the final azide concentration, yields a second-order reaction constant of $k=6.1 \pm 0.6\ mM^{-1}\ s^{-1}$, in accordance with the reaction rate that was measured by stopped flow (Table S2 in the supplementary material). On the other hand, the intercept of the fitted line with the time axis gives an estimation for the freezing time of $t_f=53 \pm 5$ ms, largely longer than the 4–5 ms reported in the manual of Bio-Logic [33].

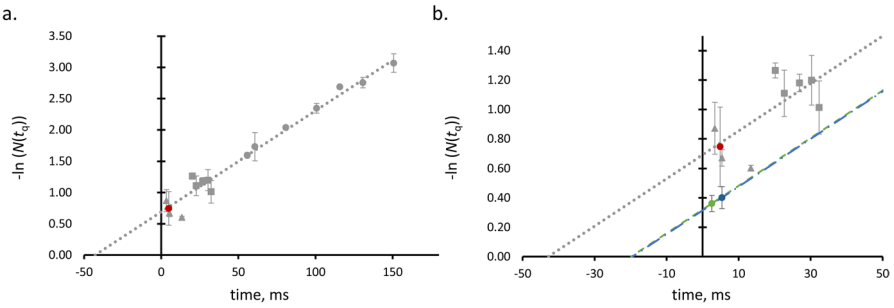

Fig. 7 **a** Plot of -ln($N(t_q)$) versus time ($=t_a+t_m+t_t$) for the calibration of RFQ system 1. An estimation of the freezing time t_f can be made from the intercept of the line with the time axis. The data points marked by a circle have been acquired varying t_a, the squares represent data with varying $t_a+t_m+t_t$ and the triangles refer to data with varying t_m+t_t achieved only through variations of the flow rate. The red circle corresponds to the result obtained with the custom-made nozzle. Each point is the average of at least three measurements and the error bars represents the standard deviation. Best fit for the equation -ln($N(t_q)$)$=k'$ $*time+q$ was found with parameters $k'=16.15 \pm 0.9\ s^{-1}$, $q=0.69 \pm 0.08$. All experiments were carried out at room temperature. **b** Zoom-in of Fig. 7a with added data points acquired using a deep isopentane bath with the standard nozzle (blue circle) and custom-made nozzle (green circle). Both samples were frozen directly into a 50 mL Falcon tube containing cold isopentane. Each point is the average of ten repetitions. The dashed green line and the dot-dashed blue line were traced parallel to the dotted line, *i.e.*, assuming the same k' as the previously described experiment and they are almost superimposed, indicating that both samples had approximately the same freezing time

In addition, a second set of samples was prepared by varying both, the flow speed (4, 5, 6, 8 and 10 mL/s) and the aging time (grey squares in Fig. 7). Again, EDL number 3 was employed. A third set of samples was prepared by only varying the flow rate (2, 5, 8 mL/s), keeping the aging time to 0 ms and using the EDL number 1 (grey triangles in Fig. 7). The quantification of the HS and LS species of ferric Mb in these samples does not even show a steady trend of increasingly higher LS concentrations when increasing the reaction time. However, both, triangles and squares are clustered not far from the linear fit of the previous dataset. Also, the ratio of HS/LS intensities was observed to vary within the same EPR tube when EPR measurements were done for different positions of the EPR tube in the resonator. We interpreted this data as having more dispersion in the freezing time between samples than the difference of the reaction times of the different data points.

In an attempt to circumvent this problem, and assuming that a narrower jet would freeze more quickly and homogenously, a custom-made EDL was manufactured with a reduced nozzle diameter of 0.3 mm instead of 0.5 mm. Unfortunately, the obtained freezing times were not shorter nor more homogeneous (see red dot in Fig. 7).

The latter experiments, however, allowed the observation that when the sample stream discharged into the isopentane, it contacts with the thermally-isolating PTFE funnel. For this reason, the depth of the isopentane freezing bath was increased to 15 cm. Using the deeper bath the reproducibility of the data improved significantly. Not only the standard deviation of each data point was reduced by approximately a factor 4 but also the homogeneity of the sample inside of the EPR tube improved considerably, since almost no difference was found in the ratio I_{HS}/I_{LS} depending on the position of the EPR tube inside the microwave cavity. Two data points acquired with the deep isopentane bath are represented with a green circle (custom-made nozzle) and a blue circle (commercial EDL #1) in Fig. 7b. To estimate the freezing time with the deep isopentane bath, a line parallel to the previous fit was traced passing through the experimental points obtained using the deep bath, since we assume *k'* will remain unaltered. The intercept with the time axis gave an estimation of the freezing time of about 20 ms. The freezing time is more than two times shorter than with the funnel but still far from the 5 ms given in the specifications of the RFQ apparatus [33].

The sample collection efficiency is quite good with this method, and the sample packing is below 70%. A volume of about 100 µL for the ejection line was considered optimum for preparation of X-band samples since the sample heights in the tube matched approximately the active volume of the resonator. With these operating conditions a minimum protein volume of over 350 µL is required to make just one sample, although part of it can be recovered from the connecting tubes after operation. If several samples are prepared, the amount of used protein per shot decreases to about 100 µL (for many samples). This is because the large dead volume of the device, due to the relatively large EDLs, mixer and, especially, the connecting lines.

4.2 Calibration of Home-Made RFQ System 2

To obtain the different calibration data points of the home-made RFQ apparatus, samples at different transport and mixing times ($t_m + t_t$) were produced by varying either the flow rate or the distance between the nozzle and the spinning rods. In both cases, the automatic discard trigger was used, the speed of rotation of the silver rods was kept constant at around 1000 rpm while the room temperature was not controlled.

The first set of calibration data were produced using an azide concentration of 4.75 mM and varying the flow rate between 32 and 93 µL/s to explore mixing and transport times between 16 and 46 ms. The freezing times t_f contained in the table were calculated by subtracting ($t_t + t_m$) from the reaction time calculated from I_{HS}/I_{LS}. The average of the t_f obtained is 46 ± 19 ms. The obtained results of HS fraction, t_q and calculated $t_m + t_t$ for every calibration sample are reported in Table 4. This dataset is significantly scattered not even showing a coherent trend.

A second set of data were acquired varying the reaction time by changing the distance of the nozzle to the silver rods and the flow rate. The concentration of azide was increased from 4.75 mM to 9.5 mM to have a faster binding reaction and an increased slope of the calibration line. This adjustment was needed to achieve a better separation between data points along the $-\ln(N(t_q))$ axis and, therefore, increased resolution in the explored time range 16 – 68 ms. The estimations of transport, quenching and freezing times for this set of calibration experiments are also reported in Table 4. Again, the estimated reaction times (t_q) were scattered and did not show a correlation with the calculated transport time. The

Table 4 Set of data collected mixing in a 1:1 volume ratio, solutions of 0.95 mM Mb and sodium azide in 50-mM TRIS buffer pH 7.8. The outlet tube was 17 mm long and the distance from the nozzle to the silver surface was kept to 25 mm except for one of the experiments for which it was 120 mm. All the experiments were performed using the mixer with frit with a volume of 0.95 µL. The quenching time was calculated from the experimental estimation of $[Mb_{HS}]$ as specified in the Methods section. The times t_m and t_t were calculated from the flow-rate

$[N_3^-]$	Flow rate	Flying distance	$t_m + t_t$	t_q	t_f*	$[Mb_{HS}]_t$
[mM]	[mL s^{-1}]	[mm]	[ms]			[% of total [Mb]]
4.75	0.093	25	16	94	78	43
	0.078	25	19	81	62	49
	0.062	25	24	70	46	54
	0.055	25	27	54	27	62
	0.047	25	31	64	33	56
	0.032	25	46	74	28	52
9.5	0.093	25	16	68	53 ± 8	30
	0.040	25	37	59	21 ± 4	35
	0.040	120	68	126	59 ± 23	11

*The average of t_f is 46 ± 19 ms and 44 ± 19 ms for $[N_3^-]$ of 4.75 mM and 9.5 mM, respectively. The second set of samples include standard deviation values as they are the average of at least two repetitions

average of t_f obtained with this set of experiments is 44 ± 19 ms, very similar to the one obtained in the previous dataset.

Despite the anticipated advantages of using spinning silver rods as freezing method, the experimental data show that this system is, in our hands, not as fast as intended in the design phase and does not reach faster freezing times than cold isopentane. Malfunction and freezing delays can be introduced in several points of the operation. First, the freezing of the sample on the silver rods takes place while the rods keep spinning and therefore the jet of sample falls at the same spot on the wheels. The thin layer of frozen material on the rods also constitutes a layer of ice that possibly reduces the good thermal conductivity of silver and acts as insulating material. Also, splashing of the mixed solution is a source of heterogeneity.

The dead volume of this mixing setup is drastically reduced to about 6 µL while the collection and packing efficiencies are comparable to the ones of the previous setup. Therefore, the minimum amount of protein solution needed to prepare one X-band EPR sample is only 56 µL, from which 50 µL goes to the sample tube.

Due to the long freezing times obtained in this calibration experiment, changes were introduced in the design and operation of the apparatus to correct these points of delay and potentially achieve faster freezing, as described below.

4.3 Calibration of Home-Made RFQ System 3

Due to the reproducibility problems encountered with RFQ system 2, the home-made mixer was combined with the deep isopentane bath whose good freezing performance was assessed with the commercial RFQ system 1. The pump setup was mounted using the mixer with no frit to avoid clogging problems which were observed with the frit after some use. The concentration of the reactants before mixing was 1 mM metmyoglobin and 30 mM sodium azide both in 50-mM TRIS buffer pH 7. The concentration of azide was increased further with respect to the previous experiments to have noticeable changes in HS metmyoglobin concentrations and therefore a better time resolution in the reaction time range of 0–20 ms. As with the previous setup, to clean the system from old, aged sample the described automatic trigger was used. Control of the reaction time was exerted by changing the length of the outlet tube in the range from 17 to 193 mm and operating at a constant flow-rate of 0.154 mL/s. The diameter of the nozzle was 0.127 mm.

The results obtained are shown in Fig. 8. Since it is hard to estimate the time needed for the reactants to mix or to freeze, the calibration line was plotted considering only the transport time t_t, calculated using Eq. 2 and therefore the intercept corresponds to $t_f + t_m$.

The reproducibility of sample preparations with this system drastically increased compared to the devices previously described. The standard deviations of the data acquired with this system are, on average, four times smaller than the standard deviation of the data collected using the commercial RFQ system 1 in the same time range. Also the homogeneity of the ratio of the EPR intensities of the HS and LS species is constant throughout the entire EPR tube, as EPR measurements done for different positions of the EPR tube in the resonator demonstrated.

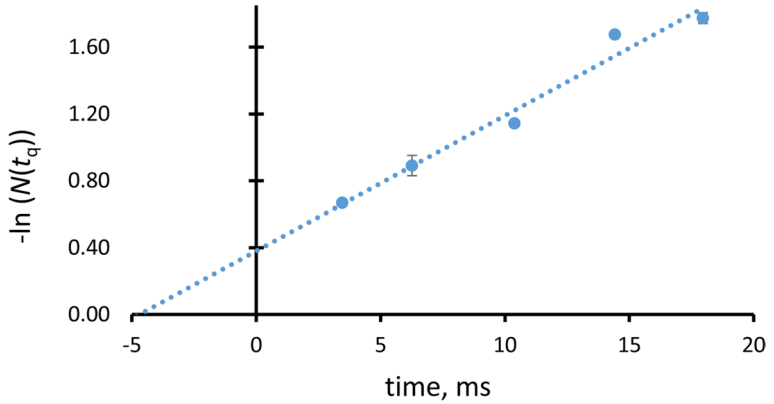

Fig. 8 Plot of -ln($N(t_q)$) versus the calculated transport time for the calibration of RFQ systems 3. The intercept of the linear fit of the data with the time-axis gives an estimate of the freezing time t_f plus mixing time t_m. Each point is the average of at least three measurements and the error bars represent the standard deviation. Best linear fit (using -ln($N(t_q)$) = k' **time* + q) was found for parameters $k' = 81.1 \pm 12.4\ s^{-1}$, $q = 0.38 \pm 0.14$. The fit has $R^2 = 0.97$

The reproducibility improvement is attributed to the use of the deep isopentane cold bath.

The best linear fit for the data points shown in Fig. 8 yields an apparent kinetic constant k' of $81.1 \pm 12.4\ s^{-1}$, which yields a kinetic constant $k = 5.4 \pm 0.8\ mM^{-1}\ s^{-1}$. This value is in perfect accordance to the value obtained by stopped-flow experiments at similar experimental conditions (see supplementary material, Table S2). This value is greatly improved with respect to the previous setups and is probably attributable to the narrower nozzle (0.127 mm) producing a very fine outlet jet. In the supplementary material (Section S3) the analysis of the data using the model of laminar flow is presented. There, the effect of friction on the transport-time heterogeneity and the aging -time distribution are analyzed. However, the differences obtained between the two models are smaller than the experimental uncertainty. With both methods, the estimation of the freezing time plus mixing time is similar. In the Fig. 8, the intercept of the fitted line with the time axis yields a value of $t_f + t_m = 4.70 \pm 1.09$ ms. The more efficient sample packing yielded better spectra with better signals so we can conclude that system 3 is our preferred apparatus, since it is faster and most inexpensive in terms of sample consumption.

To illustrate the quenching capabilities of RFQ system 3 in biological samples with highly reactive intermediates, the EPR spectrum of the freeze–quenched Compound I of the enzyme chloroperoxidase (CPO) from *Caldariomyces fumago* is shown in Fig. 9. Compound I (CPO-I) is a reactive [$Fe^{IV} = O\ Por^{\bullet+}$] species transiently formed in the CPO enzymatic cycle. Figure 9 shows the EPR spectrum of the freeze–quenched reaction product of CPO with peracetic acid (PA). It matches the EPR spectra described in literature showing a sharp peak at about $g \approx 2$ corresponding to the parallel feature of the axial powder spectrum and a broader derivative signal that is assigned to the perpendicular feature corresponding to a value of $g \approx 1.75$ of the effective g-tensor [34].

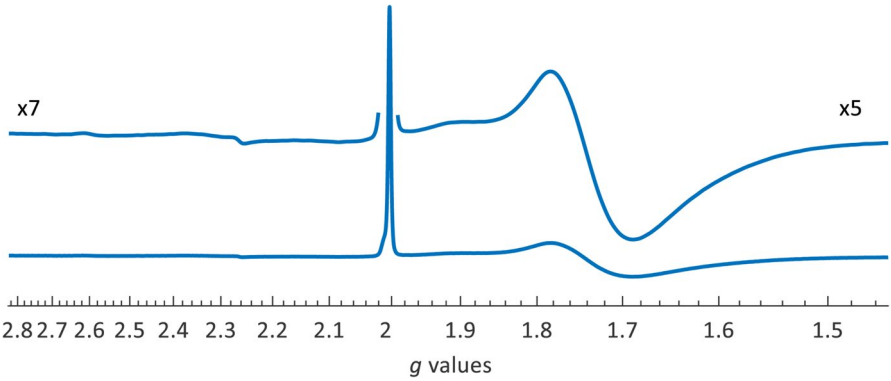

Fig. 9 X-band CW-EPR spectra of the chloroperoxidase Compound I (CPO-I) intermediate quenched at low temperature using the RFQ system 3 setup with a deep isopentane cold bath. CPO-I was obtained from the reaction of 2.5 mM CPO with 7.5 mM PA in 100 mM NaH_2PO_4 buffer (pH 4.5). EPR-measurement conditions: non-saturating microwave power of 25.19 mW, $T = 7.4$ K and modulation amplitude of 0.3 mT

5 Conclusions

Different freeze–quench devices were set up and tested for their fast-freezing abilities in the ms freezing ranges. The best results, and most economical in terms of sample consumption, were obtained using the simplest design composed of a standard syringe pump, an HPLC mixer and a deep-cold isopentane bath. Freezing times faster than 5 ms were achieved with this method. If the user is working with amounts of sample greater than 500 µL and is interested in controlling the t_q for reactions slower than 50 ms, the commercial BioLogic system with the custom-made adaptations described in Sect. 3.1. is the system of choice. If the user is interested in using a lower amount of sample or freezing the reaction in a time range faster than 20 ms, the syringe pump and the home-made mixing system is more appropriate. In both cases the deep isopentane freezing system and the use of a pump to collect the sample are highly recommended as it produces a faster and more homogenous freezing as compared to the other two freezing systems.

Supplementary Information The online version contains supplementary material available at https://doi.org/10.1007/s00723-024-01725-0.

Acknowledgements The research leading to these results received funding from the European Union's Horizon 2020 research and innovation programme under the Marie Skłodowska-Curie grant agreement No. 813209, grant No. PID2021-127287NB-I00 of the Spanish Ministry of Science and Innovation and Ayuda CEX2023-001286-S financiada por MICIU/AEI /https://doi.org/10.13039/501100011033. This study was also supported by MCIN with funding from European Union NextGenerationEU (PRTR-C17.I1) promoted by the Government of Aragon. We thank C. Obinger (University of Natural Resources and Life Sciences, Vienna) for making the BioLogic RFQ instrumentation available to us in the framework of joint projects and Oliver Oberhänsli and Reinhard Kissner (ETH Zürich) for their support in manufacturing the silver-rod freezing apparatus and Alexander Taeymans (University of Antwerp) for help in 3D printing. Also, we would like to acknowledge the use of Servicio General de Apoyo a la Investigación-SAI, Universidad de Zaragoza.

Author Contribution M. B. and I. G. R. developed the home-built RFQ Instrument. I. S., M. B. and S. V. D. developed adaptations of commercial RFQ. M. B. and I. S. performed different RFQ calibration experiments. All experiments were discussed at regular times among all authors as part of a joint H2020 Marie Skłodowska-Curie Action. All authors wrote the main manuscript text and reviewed it.

Funding H2020 Marie Skłodowska-Curie Action, 813209, Ministerio de Ciencia e Innovación, PID2021-127287NB-I00, MICIU/AEI,CEX2023-001286-S, NextGenerationEU, PRTR-C17.I1

Data Availability Data is provided within the manuscript or supplementary information files.

Declarations

Conflict of Interest The authors declare no competing interests.

References

1. R.C. Bray, Biochem. J. **81**, 189 (1961)
2. R.C. Bray, R. Pettersson, Biochem. J. **81**, 194 (1961)
3. R.E. Hansen, H. Beinert, Anal. Chem. **38**, 484 (1966)
4. D.J. Lowe, R.M. Lyndell-Bell, R.C. Bray, Biochem. J. **130**, 239–249 (1972)
5. D.P. Ballou, G.A. Palmer, Anal. Chem. **46**, 1248 (1974)
6. R.J. Appleyard, W.A. Shuttleworth, J.N.S. Evans, Biochemistry **33**, 6812 (1994)
7. A. Ivancich, H.M. Jouve, B. Sartor, J. Gaillard, Biochemistry **36**, 9356 (1997)
8. N. Ravi, J.M. Bollinger Jr., B.H. Huynh, J. Stubbe, D.E. Edmondson, J. Am. Chem. Soc. **116**, 8007 (1994)
9. S. Oellerich, E. Bill, P. Hildebrandt, Appl. Spectrosc. **54**, 1480 (2000)
10. M. Tanaka, K. Matsuura, S. Yoshioka, S. Takahashi, K. Ishimori, H. Hori, I. Morishima, Biophys. J. **84**, 1998 (2003)
11. Y. Lin, G.J. Gerfen, D.L. Rousseau, S.R. Yeh, Anal. Chem. **75**, 5381 (2003)
12. A.V. Cherepanov, S. de Vries, Biochim. Biophys. Acta—Bioenergetics **1656**, 1 (2004)
13. T. Hett, T. Zbik, S. Mukherjee, H. Matsuoka, W. Bönigk, D. Klose, C. Rouillon, N. Brenner, S. Peuker, R. Klement, H.-J. Steinhoff, H. Grubmüller, R. Seifert, O. Schiemann, U.B. Kaupp, J. Am. Chem. Soc. **143**, 6981 (2021)
14. J. Jeon, K.R. Thurber, R. Ghirlando, W.M. Yau, R. Tycko, Proc. Natl. Acad. Sci. U. S. A **116**(34), 16717 (2019)
15. N. Fehr, I. García-Rubio, G. Jeschke, H. Paulsen, Biochim. Biophys. Acta **1857**, 695 (2016)
16. T. Schmidt, J. Jeon, Y. Okuno, S.C. Chiliveri, G.M. Clore, ChemPhysChem **21**(12), 1224–1229 (2020)
17. T. Schmidt, J. Jeon, W. Yau, C.D. Schwieters, R. Tycko, G.M. Clore, PNAS (2022). https://doi.org/10.1073/pnas.2122308119
18. V. Schünemann, F. Lendzian, C. Jung, J. Contzen, A.L. Barra, S.G. Sligar, A.X. Trautwein, J. Biol. Chem. **279**, 10919 (2004)
19. J. Manzerova, V. Krymov, G.J. Gerfen, J. Magn. Reson. **213**, 32 (2011)
20. R. Kaufmann, I. Yadid, D. Goldfarb, J. Magn. Reson. **230**, 220 (2013)
21. A. Potapov, D. Goldfarb. Appl. Magn. Reson. **37**(1), 845–850 (2010)
22. E.G. Panarelli, H. van der Meer, P. Gast, E.J.J. Groenen, PLoS ONE **15**, e0232555 (2020)
23. F. Nami, P. Gast, E.J.J. Groenen, Appl. Magn. Reson. **47**, 643 (2016)
24. A.-L. Tsai, V. Berka, R.J. Kulmacz, G. Wu, G. Palmer, Anal. Biochem. **264**, 165–171 (1998)
25. Ł Bujnowicz, R. Pietras, M. Sarewicz, A. Osyczka, HardwareX **14**, e00409 (2023)
26. R. Pievo, B. Angerstein, A.J. Fielding, C. Koch, I. Feussner, M. Bennati, ChemPhysChem **14**, 4094 (2013)
27. D.R. Morris, L.P. Hager, J. Biol. Chem. **241**, 1763 (1966)
28. M.A. Pickard, Can. J. Microbiol. **27**, 1298 (1981)
29. H. Schlichting, K. Gersten, *Boundary-Layer Theory*, 9th edn. (Springer Verlag, Berlin Heidelberg, 2017), pp.416–419

30. C.Y. Lee, C.L. Chang, Y.N. Wang, L.M. Fu, Int. J. Mol. Sci. **12**, 3263 (2011)
31. T.J. Johnson, D. Ross, L.E. Locascio, Anal. Chem. **74**, 45 (2002)
32. M. El-Shahed, A. Salem, Appl. Math. Comput. **156**, 287 (2004)
33. Bio-Logic. (n.d.). *Freeze-Quench user's manual V1.6*. Retrieved 2 October 2022, from https://www.biologic.net/products/freeze-quench/
34. R. Rutter, L.P. Hager, H. Dhonau, M. Hendrich, M. Valentine, P. Debrunner, Biochemistry **23**, 6809 (1984)